Ceramics-Silikáty 66 (4), 428-435 (2022)
www.ceramics-silikaty.cz doi: 10.13168/cs.2022.0038

THE CHEMICAL ANALYSIS OF DIFFERENTLY PREPARED GLASS SURFACES – THE COMPARISON BETWEEN EDX AND XRF

#TADEÁŠ GAVENDA, ONDREJ GEDEON

Department of Glass and Ceramics, University of Chemistry and Technology, Technická 5, CZ-166 28 Prague, Czech Republic

#E-mail: gavendat@vscht.cz

Submitted June 29, 2022; accepted August 5, 2022

Keywords: Silicate glass, Glass surface, Chemical analysis, EDX, Glass corrosion

Two sets of model glasses differing by molar fractions of bridging (BO) and non-bridging (NBO) oxygens and of Q^3 and Q^4 structural units were prepared. Glasses in each set are isostructural on BO/NBO level that means the fractions of BO and NBO are the same. The groups mimic Float glass and the commercial barium crystal glass. The study compares three different ways of glass surface preparation in order to find the most realistic results of chemical analyses. The studied surfaces were: i) the original surface created by melting and exposed to the ambient atmosphere, ii) polished sample routinely prepared in way common for X-ray microanalysis, and iii) freshly fractured surface. Glasses were also analysed by XRF and the results were compared with the EDX analysis. The data suggest the EDX analysis of fresh fractures provide the most realistic composition. The comparison of XRF and EDX provide useful insight into the differences between two methods and further enhances the complexity of the glass surface study. While XRF offers a reliable analysis of bigger volume and provides averaged composition, EDX yields a more realistic surface and local composition. EDX of freshly prepared fractures revealed strong sodium enrichment on the surface due to the active participation of this element in the relaxation of the newly formed surface.

INTRODUCTION

The properties of silicate glasses is the well-studied topic as there is a huge amount of literature dealing with various aspects of silicate glasses, their properties and applications [1, 2]. Since the silicate glass is frequently used material in many industrial and special applications, it was studied in detail by a number of proven techniques and methods like scanning electron microscopy (SEM/STEM), electron probe microanalysis (EPMA), Auger electron spectroscopy (AES), Raman spectroscopy, Fourier transform infrared spectroscopy (FTIR), X-ray photoelectron spectroscopy (XPS), X-ray diffraction (XRD), nuclear magnetic resonance (NMR), molecular dynamics simulations (MD), just to name a few [3-11]. Hence, silicate glass is the thoroughly studied topic as numerous glass systems of various composition were characterized by the previously mentioned microscopic and spectroscopic methods. In addition, the knowledge of the wide range of glass properties enabled the application of plenty of empirical dependences with respect to the glass composition. However, the vast majority of the experiments and measurements were carried out on bulk samples; therefore, the obtained glass data and properties as well as empirical dependences can be fully applied only for the bulk glass samples. On the other hand, the phenomenon of the glass surface is still relatively unknown despite its significant importance. Knowledge of the glass surface is crucial since it affects the quality of the applied films and layers, determines the strength of the glass, chemical resistance, dissolution, resorption and many other optical and mechanical properties [12]. Apart from studies concerning the morphology of glass surface using AFM [13-15], the phenomenon of the glass surface (top atomic layers) in terms of chemical composition and structure is not well-documented [16]. The reasons for

the lack of detailed knowledge about glass surface (its top layer) can be expressed by the difficulty of creating an appropriate structural and chemical model of the surface and the lack of experimental surface-sensitive methods that allow us to examine the top surface layer without affecting the analysis by reaching deeper (volumetric) areas of the sample. As will be further demonstrated, the surface of the glass may be significantly different to the volume that means the volume properties cannot be simply extrapolated to the surface. As was already suggested, it is necessary to emphasize the definition of glass surface for the purpose of this study. While the term surface is commonly used in an intuitive sense as an interface between the material (glass) and the surrounding environment, it is more precise to define it as the uppermost monoatomic layer that forms a direct interface between two environments. However, this definition is questionable when it comes to amorphous solids, since it is possible to observe the continuous changes to a greater depth [17]. Hence, the surface will be used hereafter in a sense that the surface is a part of the solid with a recognizable difference from the bulk. The creation of a fresh surface results in the breakage of chemical bonds and a subsequent increase of the Gibbs energy of the surface layer, which leads to the presence of atoms with unsaturated bonds on the surface. The energy reduction on the surface begins by creating new bonds and finding new equilibrium positions of atoms. These new bonds cannot retain the three-dimensional periodicity but must be optimized with respect to the newly created interface that is realized by a number of processes, such as changing of bond lengths or bond angles. As a result of this relaxation process there are different bond lengths and angles on the glass surface as well as there are valence and coordination changes compared to the volume of glass (three-coordinated oxygen atoms and both three- and five-coordinated silicon atoms are often present on the surface of silica glass) [18, 19]. The changes in the distribution of Q-units or cycles can be expected as well [20, 21]. Generally, silicate glasses can be described as covalent-ion systems where silicon with bridging oxygen (BO) forms a basic three-dimensional network, the connectivity of which is reduced by modifiers ionically bonded to non-bridging oxygen (NBO). However, ionically bonded monovalent atoms are highly mobile in the structure and thus can actively participate in the relaxation of the newly formed surface. Hence, after the fracture of silicate glass the increase of alkali atoms can be measured on the surface [22, 23].

The differences between surface layer and the bulk raise new issues when it comes to the chemical analysis of glass. Despite the fact glass might be examined by a number of microscopic and spectroscopic methods, only few are sensitive enough to examine the chemical composition of glass in terms of the top surface layer. XPS was successfully used for the examination of glass surfaces due to its sensitivity [5]; however, Low-energy Ion Scattering spectroscopy (LEIS) is likely the method with the best sensitivity to the elemental composition of the topmost 1–2 atomic layers [16]. Among the more common methods, an energy dispersive type X-Ray detector coupled with a scanning electron microscope (often denoted as EDX) is also a suitable method for the study of glass surface as it is possible to reduce the information depth by controlling the accelerating voltage of primary electrons. Another advantage of the focused electron beam is the ability to determine the chemical composition of the sample locally. Simultaneously, as it is commonly paired with SEM, it enables correlation with the topography of materials. The chemical information then originates from the surface volume of the sample that can be decreased by using lower acceleration voltage [24]. The information depth is commonly in the range of micrometres, depending on the energy of primary electrons (and also on absorption coefficient of the analysed spectral line), but it can be decreased deeply under 1 μm by decreasing the energy of primary electrons. This feature makes EDX suitable for the surface analysis. However, the irradiation of the samples by electrons during EDX measurements may have additional side effects. A number of papers documented the volumetric and compositional changes induced by an electron beam [25-30]. The compositional changes are caused by the migration of alkali ions leaving the surface layer alkali-depleted. Hence, it may happen the amount of alkalis measured by EDX is lower than the bulk one. On the other hand, X-ray Fluorescence spectroscopy (XRF) is commonly used method for chemical analysis of glass mainly because of its relatively low cost and quickness [24]; however, the primary X-rays irradiating the sample penetrate too deep into the samples so the resulting chemical information is more volumetric and XRF cannot be considered as a suitable method for surface analysis. XRF is nevertheless considered as the standard and reliable method for checking the real composition of glass in comparison with the batch.

The main aim of this article is to focus on the surface composition of glass obtained by XRF and EDX and on changes in composition induced by different history of glass surface. Since the surface is greatly affected by its history and by the interaction with an environment, the difference between chemical composition of the original surface and the fresh fracture are expected to be significant. The fresh fracture is the surface less affected by the environment, therefore it is expected to be more suitable for the subsequent analyses; however, the presence of debris and non-planar surface might pose a challenge for the reproducibility of results. Comparison of XRF and EDX with similar theoretical accuracy [24] but with the differences in getting the corresponding X-ray spectra and therefore in their information depths might provide the interesting insight into the appropriate usage of both methods.

EXPERIMENTAL

Two series of model isostructural glass were studied in this experiment. These series mimic the commercially produced Float glass (further denoted as ACS glass) and Barium crystal glass (further denoted as ABS glass). The theoretical composition of the studied glasses is summarized in Table 1. Model glasses are close to the commercial glasses in terms of the ratio between molar amounts of bridging – n(BO) and non-bridging – n(NBO) oxygens and in terms of distribution of Q^n-motives (within a simple binary model). The structure of ACS glasses is as follows: x(BO) = 68.51 %, x(NBO) = = 31.49 % and the ratio between Q^3 and Q^4 is $x(Q^3)$ = = 74.75 %, $x(Q^4)$ = 25.25 %. On the other hand ABS glasses have a higher connectivity with values: x(BO) = = 71.96 %, x(NBO) = 28.04 %, and $x(Q^3)$ = 65.23 %, $x(Q^4)$ = 34.77 %. The ABS glasses can be therefore considered more stable due to higher degree of network connectivity. Glasses 2 and 3 belong to ACS system, the other to ABS system. Within the one system, despite the different chemical composition, the structure of silicate network (tetrahedral arrangement) remains the same.

Table 1. Molar and calculated chemical composition of glasses in weight %.

	SiO_2	Na_2O	K_2O	CaO	ZnO	MgO
Glass 1 (Na_2O·CaO 6SiO_2)	75.33	12.95		11.72		
Glass 2 (3Na_2O·3CaO 16SiO_2)	73.08	14.13		12.79		
Glass 3 (15Na_2O·6MgO·9CaO 80SiO_2)	74.14	14.34		7.78		3.73
Glass 4 (5Na_2O·K_2O 18SiO_2)	72.80	20.86	6.34			
Glass 5 (23Na_2O·ZnO 72SiO_2)	74.16	24.44			1.40	
Glass 6 (12Na_2O·11CaO ZnO 72SiO_2)	75.00	12.89		10.70	1.41	

All glasses were examined by XRD after melting in order to detect possible crystalline phases (were not detected) and subsequently samples were analysed by XRF to compare theoretical (determined by weighing of batch) and "XRF-composition". Finally, the glasses were analysed by EDX. While XRF analysis was performed on the crushed glass samples, three sets of glass samples were prepared for EDX in order to identify how the state of the surface (surface preparation, cleaning, geometry, exposure to ambient atmosphere) affects the results.

The first set consisted of samples with original surface that was created by casting the melt (further denoted as original surface – "o"). The glass samples were stored in conditions of laboratory temperature and moisture for 6 months so the surfaces were in contact with ambient atmosphere that affects the chemical composition of the surface layer. This set of samples should provide us the picture how glass surface is being changed by ambient conditions. Glass surfaces were cleaned briefly by tissue in order to remove any possible dust and then cleaned by acetone to remove any contamination. The second set (further denoted as "p") consisted of the polished samples (fractured piece of glass was fixed in the resin and polished). The samples were perfectly planar and smooth that is ideal for EDX (a flat surface is required for the plausible quantitative correction procedures); however, the analysed surface is not original anymore and the polishing process might modify the chemical composition of the surface due to the usage of liquids during the polishing process. The third set consisted of fresh fractures (further denoted as "f"). The newly created surfaces were analysed as quickly as possible after fracturing, so the interaction with ambient atmosphere was very limited. Hence, its chemical composition can be considered to be influenced only by the surface relaxation. However, there are also a few negatives of this last approach. The fresh fractures lack the ideally planar surface that is desirable for EDX and it affects the reproducibility. For this purpose, it was necessary to select among the shards those that contain flat planes of tens or hundreds of μm^2. Another difficulty was the cleaning of microscopic fragments and debris created by fracturing. It was necessary to combine multiple cleaning techniques including mechanical cleaning (by the polyester tissue) and the argon gun to blow out any remaining debris and finally cleaning by ultrasound in acetone bath to achieve the sufficiently clean surface. Of course, the whole preparation process was performed in a way the samples were minimally exposed to any contamination and their preparation times were as short as possible. The comparison between sample surfaces before and after cleaning process is presented on Figure 1.

Prepared samples were immediately measured or shortly (a few hours) kept in a vacuum chamber CY-SVC-6050 at the pressure of 1 Pa. The measurements were performed on Tescan LYRA 3 Scanning Electron Microscope equipped with EDX detector Bruker Flash 6|10 (quantification model ProZa was used). Although scanning electron microscope equipped with EDS-type detector is sometimes denoted in literature as EPMA (Electron Probe Microanalysis) the denotation EDX (Energy-dispersive X-ray spectroscopy) is quite established and will be further used in this paper. EDX measurements were performed using the accelerating voltages of 7 kV and 20 kV. All glass samples were mounted onto the aluminium holder by carbon conductive glue and coated by the thin layer of Au/Pd layer to ensure the conductivity and to avoid any charging of the samples

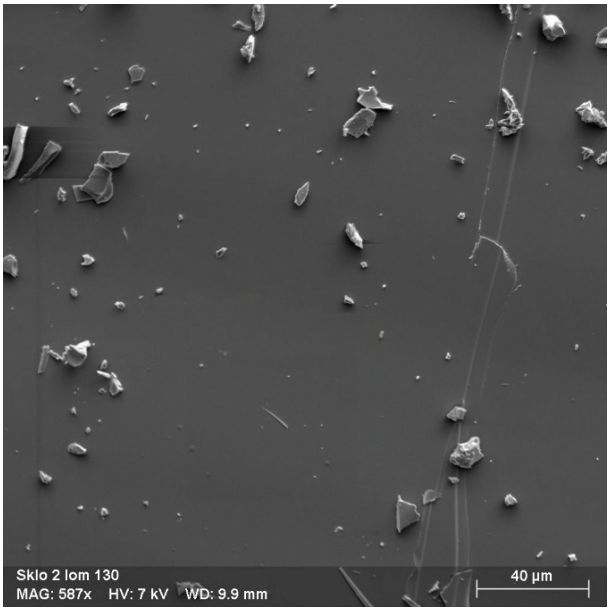

a) surface without any cleaning

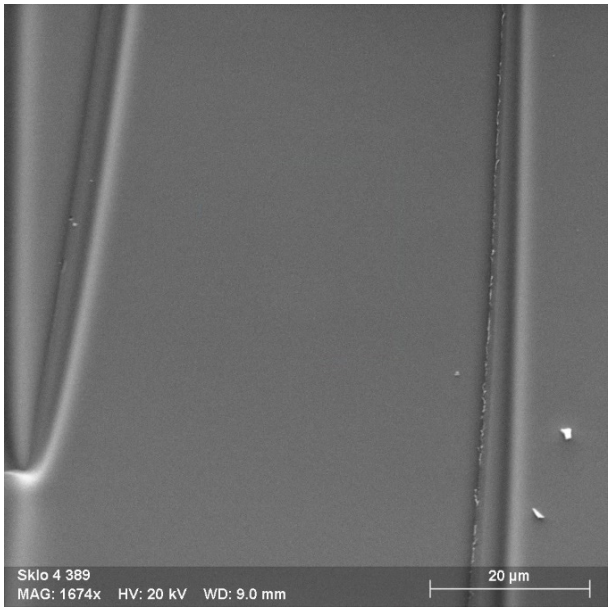

b) surface after the combination of the cleaning procedures

Figure 1. SEM images of glass sample surfaces without any cleaning (a) and b) after the combination of the cleaning procedures (mechanical, argon gun, ultrasound) show significant improvement of the surface cleanness.

(Bal-Tec SCD 500 sputter coater with a thickness monitor was used). The thickness of the metal layers was 2 nm. The samples were firstly examined by SEM in order to find an appropriate surface area without any debris. EDX analysis was performed numerous times (5-10) for each sample in order to get the statistically representative results and to eliminate the possible distant values. The analysed areas were at least 100 µm^2, large enough to minimize the alkali migration during the measurements.

RESULTS

Two different values of acceleration voltage were chosen for EDX measurements. Lower value (7 kV) decreases the information depth and therefore increases the surface sensitivity, while higher value (20 kV) enables primary electrons to reach deeper into the material. Table 2 compares the results of XRF analysis and EDX at 7 kV, while Table 3 provides a comparison between XRF and EDX using 20 kV.

The results for 7 keV show that glasses 4 and 5 containing a high amount of alkali oxides, undergo the quick corrosion even at the ambient conditions as can be deduced from the increased alkali content on the original surface. The increase of sodium content on the surface is enormous especially for glass 4. On the contrary, all polished samples indicate the decrease of sodium content in the surface layer what is attributed to the polishing process. Results for fresh fractures are apparently the closest to the theoretical composition.

The results recorded at 20 kV are in accordance with the previous measurements at 7 kV. Glasses 4 and 5 with high alkali content were already covered by a white tint that points to the almost instant corrosion at the ambient temperature. While the lower acceleration voltage (7 kV) shows increase of the alkali content due to the alkali enrichment of the surface, the higher acceleration voltage manifests the alkali decrease as the consequence of the decreased ionization probability due to the higher energy of the primary electrons (see Figure 3). Polished surfaces are similarly depleted of sodium as it was recorded at 7 kV. It is obvious that results from the fresh fractures provide the closest values with respect to theoretical composition again.

DISCUSSION

Glass samples with three different surfaces were observed in this experiment. The disadvantage of original surface lies in its exposure to the ambient conditions for a longer time-period. The glass surface is affected by humidity [31, 32] that introduces the surface corrosion [33, 34]. Glasses with higher alkali content (4 and 5) were the less stable and therefore they almost immediately reacted with atmospheric humidity. EDX measurements just confirmed this finding. The enormous amount of sodium measured at 7 kV (glass 4) is a proof of the emerging corrosion layer, while the depletion of sodium oxide measured at 20 kV is expandable with this inhomogeneous alkali distribution, see Figure 3. Actually, original surfaces of all glasses were covered by a certain amount of the corrosion products, however, the effect was far more pronounced for the unstable glasses 4 and 5 containing more alkali oxides (Figure 2).

Table 2. Results of XRF and EDX analysis compared with the theoretical chemical composition (denoted as "Theor"). EDX results are obtained at accelerating voltage of 7 kV. The abbreviations stand for: o – original surface, p – polished sample, f – fresh fracture. The errors correspond to 1σ statistical variation.

		SiO_2	Na_2O	K_2O	CaO	ZnO	MgO
1	Theor	75.33	12.95		11.72		
	XRF	73.7	13.3		13.0		
	EDX o	76.4 ± 0.3	11.9 ± 0.2		11.7 ± 0.2		
	EDX p	75.2 ± 0.4	12.0 ± 0.2		12.8 ± 0.3		
	EDX f	76.7 ± 0.4	12.0 ± 0.2		11.3 ± 0.3		
2	Theor	73.08	14.13		12.79		
	XRF	71.6	14.5		13.9		
	EDX o	76.1 ± 0.3	12.8 ± 0.1		11.1 ± 0.4		
	EDX p	75.7 ± 0.4	12.6 ± 0.2		11.7 ± 0.4		
	EDX f	74.6 ± 0.8	13.3 ± 0.4		12.1 ± 0.5		
3	Theor	74.14	14.34		7.78		3.73
	XRF	73.2	14.5		8.3		4.0
	EDX o	75.1 ± 0.3	13.7 ± 0.2		7.4 ± 0.3		3.8 ± 0.1
	EDX p	76.1 ± 0.2	13.0 ± 0.2		7.2 ± 0.1		3.7 ± 0.1
	EDX f	74.9 ± 0.5	13.8 ± 0.3		7.4 ± 0.2		3.9 ± 0.1
4	Theor	72.80	20.86	6.34			
	XRF	72.8	21.1	6.1			
	EDX o	40.7 ± 5.4	56.6 ± 6.1	2.7 ± 0.9			
	EDX p	77.0 ± 0.4	17.8 ± 0.4	5.2 ± 0.2			
	EDX f	75.0 ± 0.4	19.9 ± 0.4	5.1 ± 0.1			
5	Theor	74.16	24.44			1.40	
	XRF	73.8	24.5			1.7	
	EDX o	70.7 ± 1.9	27.3 ± 1.90			2.0 ± 0.2	
	EDX p	78.6 ± 0.2	19.3 ± 0.3			2.1 ± 0.2	
	EDX f	76.5 ± 0.9	21.9 ± 0.8			1.6 ± 0.1	
6	Theor	75.00	12.89		10.70	1.41	
	XRF	73.5	13.0		11.9	1.6	
	EDX o	75.4 ± 0.2	13.0 ± 0.2		10.4 ± 0.2	1.2 ± 0.2	
	EDX p	74.9 ± 0.4	12.0 ± 0.3		11.4 ± 0.5	1.7 ± 0.4	
	EDX f	75.4 ± 0.4	12.4 ± 0.2		11.0 ± 0.4	1.2 ± 0.1	

Table 3. Results of XRF and EDX analysis compared with theoretical chemical composition (denoted as "Theor"). The acceleration voltage for EDX was set to 20 kV. The abbreviations stand for: o – original surface, p – polished sample, f – fresh fracture. The errors correspond to 1σ statistical variation.

		SiO_2	Na_2O	K_2O	CaO	ZnO	MgO
1	Theor	75.33	12.95		11.72		
	XRF	73.7	13.3		13.0		
	EDX o	77.8 ± 0.5	10.7 ± 0.2		11.5 ± 0.4		
	EDX p	75.4 ± 0.3	11.2 ± 0.2		13.4 ± 0.2		
	EDX f	76.0 ± 0.5	12.3 ± 0.6		11.7 ± 0.7		
2	Theor	73.08	14.13		12.79		
	XRF	71.6	14.5		13.9		
	EDX o	76.4 ± 0.1	12.3 ± 0.1		11.3 ± 0.1		
	EDX p	75.7 ± 0.3	11.8 ± 0.1		12.5 ± 0.3		
	EDX f	73.9 ±0.7	13.8 ± 0.3		12.3 ± 0.6		
3	Theor	74.14	14.34		7.78		3.73
	XRF	73.2	14.5		8.3		4.0
	EDX o	76.4 ± 0.1	12.5 ± 0.1		7.5 ± 0.1		3.6 ± 0.1
	EDX p	76.8 ± 0.1	11.7 ± 0.1		8.0 ± 0.1		3.5 ± 0.1
	EDX f	75.5 ± 0.4	13.5 ± 0.6		7.1 ± 0.3		3.9 ± 0.1
4	Theor	72.80	20.86	6.34			
	XRF	72.8	21.1	6.1			
	EDX o	81.1 ± 0.5	13.3 ±0.5	5.6 ±0.1			
	EDX p	76.8 ± 0.2	17.9 ± 0.2	5.3 ± 0.1			
	EDX f	75.1 ± 0.2	20.0 ± 0.2	4.9 ± 0.1			
5	Theor	74.16	24.44			1.40	
	XRF	73.8	24.5			1.7	
	EDX o	79.8 ± 0.3	18.6 ± 0.3			1.6 ± 0.1	
	EDX p	77.8 ± 0.4	20.8 ± 0.4			1.4 ± 0.1	
	EDX f	75.8 ± 0.7	22.7 ± 0.7			1.5 ± 0.1	
6	Theor	75.00	12.89		10.70	1.41	
	XRF	73.5	13.0		11.9	1.6	
	EDX o	76.4 ± 0.1	12.9 ± 0.1		9.5 ± 0.1	1.2 ± 0.1	
	EDX p	74.3 ± 0.4	12.0 ± 0.1		11.9 ± 0.2	1.8 ± 0.2	
	EDX f	76.0 ± 0.4	12.6 ± 0.5		10.1 ± 0.5	1.3 ± 0.2	

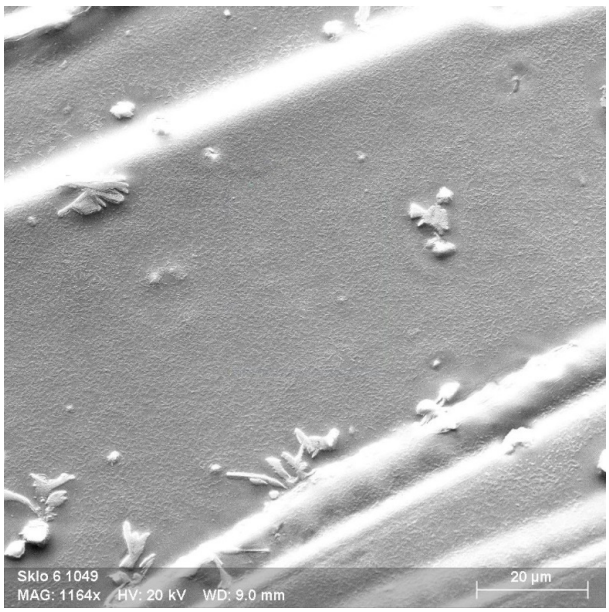

Figure 2. SEM image of the original surface of Glass 5, fully covered by corrosion products that create a white tint visible by a naked eye.

The original surface cannot be used for a reliable analysis, because the topmost surface is enriched with alkalis altering the composition in comparison to the bulk.

The advantage of polished samples was their smooth surface (ideal for EDX) that resulted in the smallest value of the standard deviation; therefore, this way of surface preparation is ideal for reproducibility. However, the polishing commonly includes the usage of water that causes removal of alkalis from the surface. The alkali depletion apparently reaches deeper areas as even analyses performed at 20 kV show lower values of sodium content (lower than at original surface). It is apparent that polishing modifies the surface.

Finally, fresh fractures seem to provide the most realistic analyses as the newly created surface can be quickly measured without being significantly affected by atmosphere and humidity. Indeed, the amount of Na_2O measured by EDX on fresh fractures is almost in all cases the closest to the theoretical values. Thus, to get the correct composition, it seems more appropriate to use fresh fractures instead of the polished glass. Nevertheless, analyses on fractures require more experience that includes a careful selection of the analysed area, thoroughgoing cleaning and preparation of samples. The analyses cannot be therefore easily standardized. EDX analyses on fresh fractures show the largest statistical variance that is just due to the uncertainty of the tilt angles on the measured areas (although some almost planar areas can be found on most samples). The effect of uneven surface can be suppressed by increasing the energy of primary electrons. Increase of the energy of the primary electrons from 7 to 20 kV increases their range approximately eight times that will result in less sensitivity on the surface inclination [24]. The results obtained at higher accelerating voltage also manifest the alkali decrease. This decrease is virtual and can be explained by the decreased ionization probability caused by higher energy of the primary electrons. The electron irradiation generally causes the emission of X-ray photons, which is preceded by the ionization of the particular atomic layer [24]. Figure 3 presents the depth distribution of ionization $\Phi(z)$ that has a typical shape (curve 3) that depends on the scattering of bombarding electrons in solid and the course of ionization cross-section on the energy. Emitted X-ray photons are proportional to the number of ionized atoms and the amount of photons detected in the depth z is, of course, dependent on X-ray absorption. If the absorption is negligible, the shape of the emission function $n(z)$ is identical with the function $\Phi(z)$. The emission function n(z) indicates the contribution of photons in the depth z to the overall amount of detected photons, thus its integral gives the overall amount of detected X-ray photons. Figure 3 shows what may happen when the composition in the analysed volume area is changed. The black bars represent the original place of atoms, while the grey ones stand for their new locations. Situation A (move of alkalis deep in the interaction volume) shows the analytical signal for emission curves 2 and 3 increases but the alkali move cannot affect the curve 1. Situation B (move of alkalis close to the maximum of $\Phi(z)$) causes the signal increase for the curve 2, but the signals corresponding to the curves 1 and 3 remain unchanged. Finally, the situation C (move of alkalis close the surface) causes the increase of the signal for the curve 1 and decreases of signals for the curves 2 and 3. The case C corresponds to the common migration of alkalis onto glass surface. It is seen that depending on the particular situation, the intensity can be anticorrelated with concentration and therefore may cause the wrong interpretation, when the

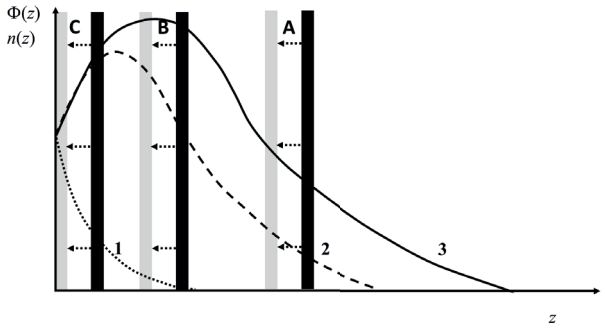

Figure 3. The typical distribution of ionizations in a sample, $\Phi(z)$ and the corresponding emission distribution curves of X-ray photons, n(z), influenced by various absorption values. The curve 3 corresponds to the emission distribution function with zero (negligible) absorption of X-ray radiation. The curve 2 is attributed to the case of a low absorption, while the curve 1 demonstrates the example of a high absorption coefficient.

decreased intensity of the particular element is explained as a decrease of its surface concentration instead of its real increase.

XRF and EDX provide the different analytical results. To explain this it is necessary to focus more on the principles of both methods and their specific features. The accuracy of both methods is approximately comparable (1 rel. %). However, the electron beam used in EDX can be focused to the micrometre scale. In addition, the lateral resolution of the EDX is around one micrometre. It means that EDX can be also used to assess the lateral homogeneity of the glass and the chemical changes on the surface. Although the information depth is in the order of micrometres (depends on the sample density and can be significantly reduced by decreasing the energy of the primary electrons), high sensitivity of the method enables to observe changes of the surface composition. On the other hand, XRF provides the chemical analysis of larger volumes and the method is not surface sensitive. Hence, XRF was expected to provide results closer to the theoretical chemical composition, while the results obtained by EDX were assumed to be different mainly for Na2O content as sodium is involved in the surface relaxation. A brief look at Table 2 shows that the XRF method systematically underestimates the SiO_2 content that causes the higher content of the other oxides in the XRF results. On the contrary, EDX measurements performed at the lower accelerating voltage (7 kV) are very surface sensitive (the information depth can be estimated to around 1 μm) which results in significantly different values in comparison with XRF. Hence, EDX analyses performed at the higher accelerating voltage (20 kV) seem to be a reasonable compromise as they are most likely the closest to the correct values. Results presented in Table 3 indeed demonstrate the values obtained at 20 kV are generally shifted closer to theoretical values. However, this also means that deviations between the results at 7 kV and 20 kV can be partly attributed to the real differences between volume and surface composition.

If we focus primarily on alkalis, where the largest differences are expected, then the alkali content was shifted systematically to higher values for XRF. The absolute comparison between the theoretical composition and EDX shows the match within the statistical reliability 2σ for glasses 1-3 and 6; the lower alkali content for glasses 4 and 5 can be partly attributed to the loss during melting. The values, in contradiction to XRF, were never higher than the theoretical value. This shows that EDX yield more realistic results than XRF, which systematically overestimates the alkali content and gives higher values than theoretical ones. Considering that alkalis are the most volatile part in glass, the results of EDX, unlike XRF, are quite consistent with this fact. An overall comparison of XRF and EDX confirms that both methods have comparable accuracy, but EDX results appear to be more consistent in this case, see Na_2O deviations. In addition, EDX offers the possibility of volume and surface analysis and, of course, locality, which is invaluable when measuring small objects.

CONCLUSIONS

Presented study provides the comparison between three different methods of glass surface preparation – the original surface, the polished sample and the fresh fracture. The original surface was affected by the ambient environment that resulted in the corrosion processes leading to the change of chemical composition. The polished surfaces proved ideal for X-ray microanalysis in terms of surface smoothness and showed the smallest statistical deviations; however, the surface chemical composition was affected by polishing process resulting in the depletion of alkalis. The measurements on the fresh fractures yielded the most satisfactory values because the measured chemical composition of the surface is significantly closer to the theoretical composition. Nevertheless, the preparation of fresh fractures for chemical analysis is not trivial but requires a careful manipulation and cleaning to reach reasonable statistical deviations. Glass samples were also analysed by XRF and their comparison with EDX shows a systematic overestimation of the alkali content by XRF, while the EDX results seem to be more consistent and realistic.

Acknowledgement

This research was funded by the MSMT (Ministry of Education, Youth, and Sports) of the Czech Republic, grant number LTT20001 in the scheme INTER-TRANSFER.

REFERENCES

1. Bansal N. P., Doremus R. H. (1986). Handbook of Glass Properties. Academic Press, Inc.
2. Mazurin O. V., Streltsina M. V., Shvaiko-shvaikovskaya T. P. (1983). Handbook of Glass Data. Elsevier.
3. Nakazawa K. et al. (2018): Identification of nanometer-scale compositional fluctuations in silicate glass using electron microscopy and spectroscopy. *Scripta Materialia, 154*, 197-201. doi:10.1016/j.scriptamat.2018.05.048
4. Rahier H., Simons W., Van Mele B., Biesemans M. (1997): Low-temperature synthesized aluminosilicate glasses: Part III Influence of the composition of the silicate solution on production, structure and properties. *Journal of Materials Science, 32*, 2237-2247. doi:10.1023/A:1018563914630
5. Zemek J., Jiricek P., Gedeon O., Lesiak B., Jozwik A. (2005): Electron irradiated potassium-silicate glass surfaces investigated by XPS. *Journal of Non-Crystalline Solids, 351*, 1665-1674. doi:10.1016/j.jnoncrysol.2005.04.059
6. Moulton B. J. A. et al. (2022): A critical evaluation of

barium silicate glass network polymerization. *Journal of Non-Crystalline Solids, 583*, 121477. doi:10.1016/j.jnoncrysol.2022.121477
7. Ollier N., Gedeon O. (2006): Micro-Raman studies on 50 keV electron irradiated silicate glass. *Journal of Non-Crystalline Solids, 352*, 5337-5343. doi:10.1016/j.jnoncrysol.2006.08.026
8. Strugaj G., Herrmann A., Radlein E. (2021): AES and EDX surface analysis of weathered float glass exposed in different environmental conditions. *Journal of Non-Crystalline Solids, 572*, 121083. doi:10.1016/j.jnoncrysol.2021.121083
9. Jabraoui H. et al. (2016): Molecular dynamics simulation of thermodynamic and structural properties of silicate glass: Effect of the alkali oxide modifiers. *Journal of Non-Crystalline Solids, 448*, 16-26. doi:10.1016/j.jnoncrysol.2016.06.030
10. Jurek K., Gedeon O. (2003): Analysis of alkali–silicate glasses by electron probe analysis. *Spectrochimica Acta Part B: Atomic spectroscopy, 58*(4), 741-744. doi:10.1016/S0584-8547(02)00288-4
11. Lacharme J. P., Champion P., Leger D. (1981): Auger electron spectroscopy on fractured glass surface. *Scanning Electron Microscopy, 1*, 237-243.
12. Yanik M. C. O. et al. (2018): Influence of different process conditions on mechanical, optical and surface properties of silver ion exchanged soda-lime silicate glass. *Journal of Non-Crystalline Solids, 493*, 1-10. doi:10.1016/j.jnoncrysol.2018.04.024
13. Gedeon O., Jurek K., Drbohlav I. (2007): Changes in surface morphology of silicate glass induced by fast electron irradiation. *Journal of Non-Crystalline Solids, 353*, 1946-1950. doi:10.1016/j.jnoncrysol.2007.01.058
14. Hopf J., Pierce E., M. (2014): Topography and mechanical property mapping of international simple glass surfaces with atomic force microscopy. *Procedia Materials Science, 7*, 216-222. doi:10.1016/j.mspro.2014.10.028
15. Raberg W., Ostadrahimi A., H., Kayser T., Wandelt K. (2005): Atomic scale imaging of amorphous silicate glass surfaces by scanning force microscopy. *Journal of Non-Crystalline Solids, 351*,1089-1096. doi:10.1016/j.jnoncrysol.2005.01.022
16. Almeida R. M., Hickey R., Himanshu J., Pantano C. G. (2014): Low-energy ion scattering spectroscopy of silicate glass surfaces. *Journal of Non-Crystalline Solids, 385*, 124-128. doi:10.1016/j.jnoncrysol.2013.11.020
17. Pintori G., Cattaruzza E. (2022): XPS/ESCA on glass surfaces: A useful tool for ancient and modern materials. *Optical Materials: X*, 13, 100108. doi:10.1016/j.omx.2021.100108
18. Machacek J., Gedeon O., Liska M. (2022): Comparison of silica and sodium trisilicate glass surfaces created by moulding and breaking - MD simulation. *Ceramics-Silikáty, 66*, 43-53. doi:10.13168/cs.2021.0051
19. Frischat G. H., Poggemann J. F., Heide G. (2004): Nanostructure and atomic structure of glass seen by atomic force microscopy. *Journal of Non-Crystalline Solids, 345 – 346*, 197-202. doi:10.1016/j.jnoncrysol.2004.08.022
20. Gedeon O. (2018): Medium range order and configurational entropy of vitreous silica. *Physics and Chemistry of Glasses-European Journal of Glass Science and Technology Part B, 59* (1), 27-33. doi:10.13036/17533562.59.1.007
21. Gedeon O., Liska M., Machacek J. (2008): Connectivity of Q-species in binary sodium-silicate glasses. *Journal of Non-Crystalline Solids, 354* (12-13), 1133-1136. doi:10.1016/j.jnoncrysol.2006.11.028
22. Zemek J., Gedeon O.(2004): Potassium surface enrichment in mixed alkali glass irradiated with electrons. *Journal of Non-Crystalline Solids, 337*, 268-271. doi:10.1016/j.jnoncrysol.2004.04.025
23. Gedeon O., Zemek J. (2003): Low energy and low dose electron irradiation of potassium-lime-silicate glass investigated by XPS. I. Surface composition. *Journal of Non-Crystalline Solids, 320*, 177-186. doi:10.1016/S0022-3093(03)00015-2
24. Leng Y. (2013). *Materials Characterization: Introduction to Microscopic and Spectroscopic Methods.* 2nd Ed. Wiley, pp. 1-376. doi:10.1002/9783527670772
25. Gavenda T., Gedeon O., Jurek K. (2017): Structural and volume changes and their correlation in electron irradiated alkali silicate glasses. *Nuclear Instruments and Methods in Physics Research Section B: Beam Interactions with Materials and Atoms, 397*, 15-26. doi:10.1016/j.nimb.2017.02.026
26. Gavenda T., Gedeon O., Jurek K. (2014): Volume changes in glass induced by an electron beam. *Nuclear Instruments and Methods in Physics Research Section B: Beam Interactions with Materials and Atoms, 322*, 7-12. doi:10.1016/j.nimb.2013.12.017
27. Gedeon O., Jurek K., Drbohlav I., Ollier N. (2009): Binary potassium-silicate glass irradiated with electrons. *Nuclear Instruments and Methods in Physics Research Section B: Beam Interactions with Materials and Atoms, 267* (20), 3461-3465. doi:10.1016/j.nimb.2009.07.022
28. Gedeon O., Jurek K., Drbohlav I. (2010): Mixed-alkali effect in sodium-potassium glasses irradiated with electrons. *Journal of Non-Crystalline Solids, 356*, 456-460. doi:10.1016/j.jnoncrysol.2009.12.010
29. Jurek K., Gedeon O. (2008): Volume and composition surface changes in alkali silicate glass irradiated with electrons. *Microchimica Acta, 161*, 377-380. doi:10.1007/s00604-008-0941-1
30. Jurek K., Gedeon O. (2021): Potassium-silicate glass foil irradiated with electrons – Asymmetry in migration and space distribution given by the elastic scattering of electrons on potassium atoms. *Nuclear Instruments and Methods in Physics Research Section B: Beam Interactions with Materials and Atoms, 502*, 150-156. doi:10.1016/j.nimb.2021.06.017
31. Alloteau F. et al. (2019): Temperature-dependent mechanisms of the atmospheric alteration of a mixed-alkali lime silicate glass. *Corrosion Science, 159*, 108129. doi:10.1016/j.corsci.2019.108129
32. Melcher M., Schreiner M. (2013). *Glass degradation by liquids and atmospheric agents. Modern methods for analysing archaeological and historical glass*. Wiley, pp. 608-651. doi:10.1002/9781118314234.ch29
33. Galusková D., Galusek D. (2021): Corrosion and degradation of glass. In: *Encyclopedia of Materials: Technical Ceramics and Glasses, 1*, 932-940. doi:10.1016/B978-0-12-818542-1.00069-2
34. Chopinet M. H. et al. (2008): Soda-lime-silica glass containers: Chemical durability and weathering products. *Advanced Materials Research, 39 – 40*, 305-310. doi:10.4028/www.scientific.net/AMR.39-40.305